

The Interstellar Rubidium Isotope Ratio toward Rho Ophiuchi A

S.R. Federman^{1,2}, David C. Knauth³, and David L. Lambert⁴

ABSTRACT

The isotope ratio, $^{85}\text{Rb}/^{87}\text{Rb}$, places constraints on models of the nucleosynthesis of heavy elements, but there is no precise determination of the ratio for material beyond the Solar System. We report the first measurement of the interstellar Rb isotope ratio. Our measurement of the Rb I line at 7800 Å for the diffuse gas toward ρ Oph A yields a value of 1.21 ± 0.30 ($1-\sigma$) that differs significantly from the meteoritic value of 2.59. The Rb/K elemental abundance ratio for the cloud also is lower than that seen in meteorites. Comparison of the $^{85}\text{Rb}/\text{K}$ and $^{87}\text{Rb}/\text{K}$ ratios with meteoritic values indicates that the interstellar ^{85}Rb abundance in this direction is lower than the Solar System abundance. We attribute the lower abundance to a reduced contribution from the *r*-process. Interstellar abundances for Kr, Cd, and Sn are consistent with much less *r*-process synthesis for the solar neighborhood compared to the amount inferred for the Solar System.

Subject headings: ISM: abundances — ISM: atoms — star: individual (ρ Oph A)

1. Introduction

Studies on rubidium in stellar atmospheres and the interstellar medium (ISM) are few, but it is not for a lack of interest in its abundance. The production of Rb involves the neutron capture *s*- and *r*-processes. Rubidium production by the *s*-process occurs through the ‘weak’ process in the He- and C-burning layers of massive stars and through the ‘main’ process in the He-shell of low-mass AGB stars. Supernovae from core collapse of massive stars are the

¹Department of Physics and Astronomy, University of Toledo, Toledo, OH 43606; sfederm@uoft02.utoledo.edu.

²Guest Observer, McDonald Observatory, University of Texas at Austin.

³Department of Physics and Astronomy, The Johns Hopkins University, 3400 North Charles Street, Baltimore, MD 21218; dknauth@pha.jhu.edu.

⁴Department of Astronomy, University of Texas, Austin, TX, 78712; dll@astro.as.utexas.edu.

likely source of the *r*-process. Analysis of the Solar System abundances provides estimates of the fractional responsibility of these neutron capture processes for the Rb isotopes ^{85}Rb and ^{87}Rb . Our estimates drawn from averaging the results of Beer, Walter, & Käppeler (1992), Raiteri et al. (1993), and Arlandini et al. (1999) are that ^{85}Rb is about 35% *s*- and 65% *r*-process in origin with the weak *s*-process being one third of the *s*-process contribution. For ^{87}Rb , the fractions are about 70% from the *s*- and 30% from the *r*-process with a minor contribution from the weak *s*-process. As a result of the different relative contributions of the *s*- and *r*-processes to the two isotopes, a measurement of the Rb isotope ratio is a clue to the history of heavy element nucleosynthesis.

Unfortunately, rubidium is a difficult element to measure. It is potentially measureable only in cool stars. Resonance lines of Rb I are detectable at 7800 and 7947 Å, but blending with atomic and/or molecular lines adds an unwelcome difficulty to an abundance analysis. Rubidium abundances for unevolved stars were reported by Gratton & Sneden (1994) and Tomkin & Lambert (1989). Measurements of the abundance for giant stars were obtained by Lambert et al. (1995), Abia & Wallerstein (1998), and Abia et al. (2001). The primary aim of these latter studies was to exploit the use of Rb as a neutron densitometer for the *s*-process site (Lambert et al. 1995). This use arises from the role of ^{85}Kr as a branch in the *s*-process path. The branch directly affects the isotope ratio, $^{85}\text{Rb}/^{87}\text{Rb}$, but it is not directly measureable from even very high resolution stellar spectra (Lambert & Luck 1976) because the lines are too broad. Earlier interstellar measurements yielded upper limits (Federman et al. 1985) because the Rb abundance is quite small (2.5×10^{-10} in meteorites; Anders & Grevesse 1989), and it is derived from Rb I, not the dominant form Rb II. The only interstellar detection so far comes from observations on two heavily reddened stars in Cygnus (Gredel, Black, & Yan 2001). [An earlier reported detection by Jura & Smith (1981) could not be confirmed by Federman et al. (1985).] Here, we present high-resolution spectra revealing not only another interstellar detection, but also the first measurement determining the $^{85}\text{Rb}/^{87}\text{Rb}$ isotope ratio for extrasolar gas.

2. Observations and Analysis

The star ρ Oph A is an ideal target for a study on Rb isotopes. It is relatively bright ($V = 5.0$), moderately reddened with $E(B-V) = 0.47$, and has one main interstellar component (e.g., Lemoine et al. 1993). The weak lines of Li I (Lemoine et al. 1993) and K I $\lambda 4044$ (Crutcher 1978) toward this star also show more absorption than is typical for a diffuse cloud.

The data on Rb I $\lambda 7800$ were acquired with the 2dcoudé spectrograph (Tull et al. 1995)

on the Harlan J. Smith 2.7 m telescope at McDonald Observatory in 2003 May. We used the high-resolution mode with echelle grating E2, centered on 7444 Å in order 46. The spectra were imaged onto a 2048×2048 Tektronics CCD (TK3). The $145 \mu\text{m}$ slit provided a resolving power of 175,000 as determined from widths of lines in the Th-Ar comparison spectrum, sufficient to discern broadening of the interstellar lines. We obtained calibration exposures for dark current the first night of the run, bias correction and flat fielding each night, and Th-Ar spectra every 2 to 3 hours during the night. Our primary target, ρ Oph A, was observed for a total of 8^h , with individual exposures of 30^m per frame; this procedure minimized the deleterious effects caused by cosmic rays. In addition, the unreddened star α Vir was observed for a total of 100^m centered on the slit to check for contamination from weak telluric lines and CCD blemishes not removed during the flat-fielding process. No contamination is present. An additional 60^m was utilized to trail α Vir along the slit to act as a stellar flat field. The analysis described below utilized spectra of the K I line at 4044 Å that were acquired for another project (Knauth, Federman, & Lambert 2004). While details will be presented in Knauth et al. (2004), we note that the instrumentation and observing procedure were basically the same as those for Rb I, except echelle grating E1 was used. There is at most a 0.1 km s^{-1} difference in line velocities between the two setups according to the dispersion solutions found from Th-Ar spectra.

Standard routines within the IRAF environment were used to extract one-dimensional spectra that were Doppler-corrected and normalized to unity. The Rb I spectrum for the interstellar gas toward ρ Oph A is displayed in Fig. 1. The appearance of two ‘features’ arises from the $62 \text{ m}\text{\AA}$ hyperfine splitting in ^{85}Rb combined with the stronger (redder) hyperfine component in ^{87}Rb . The rms deviations in the stellar continuum yield a signal-to-noise ratio per pixel of 1200 for ρ Oph A; there are 2.9 pixels per resolution element.

As in our earlier work on the Li isotope ratio acquired at the same resolution (Knauth et al. 2000), the Rb I and K I lines were fitted to extract column densities for neutral ^{85}Rb , ^{87}Rb , and K. The relevant atomic data used for input (Morton 1991, 2000) and the resulting equivalent widths (W_λ) and column densities (N) are given in Table 1. There is one main component at V_{LSR} of 1.9 km s^{-1} (Lemoine et al. 1993; Pan et al. 2003), which at ultra-high-resolution is seen as two in K I $\lambda 7699$ spectra (Welty & Hobbs 2001). Another component at 3.5 km s^{-1} appears in K I $\lambda 7699$ (Welty & Hobbs 2001; Pan et al. 2003), having $\approx 20\%$ of the column of the main component. This second component is marginally seen (at the 2σ level) in our K I $\lambda 4044$ spectrum, but there is no evidence for it in the Rb I line. The uncertainties in column densities were inferred from a map of chi-squared confidence levels (Fig. 2). While optical depth effects are not important for these very weak lines, the profile fitting code (see Knauth et al. 2003) determines the b -value as well (from the difference between measured line width and the instrumental width determined from Th-Ar

lines). We obtained b -values of 1.0 and 0.8 km s^{−1} for Rb I and K I; the slight difference is not significant at our spectral resolution.

3. Results

The primary result of our study is the determination of a Rb isotope ratio for the main cloud toward ρ Oph A. The best fit (with a reduced chi squared of 1.43 for 47 degrees of freedom) yields a $^{85}\text{Rb}/^{87}\text{Rb}$ ratio of 1.21 ± 0.30 – see top panel of Fig. 1. This differs significantly from the meteoritic value of 2.59 (Anders & Grevesse 1989). We attempted to fit our data with the Solar System ratio as well (bottom panel of Fig. 1). The reduced chi squared is worse (2.08) and an F-test shows that there is 50% confidence in this fit. Examination of the lower panel reveals where the difference lies: Neither the blue nor red shoulders of the lines are fit well using a Solar System ratio. Furthermore, the goodness of fit can be judged by variations in the residuals (data minus fit) outside and inside the absorption profile. The variation in the lower panel is not as consistent across the spectrum. Other syntheses with the Solar System ratio were attempted without success. Because both shoulders show more absorption than is predicted by this ratio, addition of the redder 3.5 km s^{−1} component would not improve the fit. Broader lines could fill in the shoulders of the observed Rb I profile, as could a two-component fit upon shifting the profile by about 1 resolution element. [A b -value as large as 1.8 km s^{−1} is possible from our χ^2 analysis, though it is not consistent with other data (e.g., Welty & Hobbs 2001).] However, the ^{85}Rb hyperfine components are broadened as well, yielding a chi squared that is almost double the χ^2 of the best fit in both cases. Finally, we note that the lines representing different values of $^{85}\text{Rb}/^{87}\text{Rb}$ in Fig. 2 favor a ratio between 1.0 and 1.5. The Solar System ratio of 2.6 differs by 2- to 3- σ in each quantity (column of Rb isotope), consistent with the 4.5- σ difference seen in the uncertainty listed for the $^{85}\text{Rb}/^{87}\text{Rb}$ ratio.

The Rb/K elemental ratio provides a means to determine for this interstellar cloud whether the ^{85}Rb abundance is lower or the ^{87}Rb abundance is higher relative to the abundances in meteorites. Since Rb I and K I are minor interstellar species, ionization balance is required to extract an elemental abundance. The elemental ratio does not depend on electron density, and we assume that the depletion levels for alkalis are the same (see Welty & Hobbs 2001; Knauth et al. 2003). Then for the Rb/K ratio, we have

$$\frac{A_g(\text{Rb})}{A_g(\text{K})} = \left[\frac{N(\text{Rb I})}{N(\text{K I})} \right] \left[\frac{G(\text{Rb I})}{G(\text{K I})} \right] \left[\frac{\alpha(\text{K I})}{\alpha(\text{Rb I})} \right], \quad (1)$$

where $G(X)$ is the photoionization rate corrected for grain attenuation and $\alpha(X)$ is the

rate coefficient for radiative recombination. Comparison of the theoretical calculations for radiative recombination of Rb and K (Wane 1985; Péquignot & Aldrovandi 1986; Wane & Aymar 1987) reveals that the coefficients are the same to within about 10%, confirming the assumption made in other interstellar studies (Jura & Smith 1981; Federman et al. 1985; Gredel et al. 2001). The photoionization rates for Rb I and K I are 3.42×10^{-12} and $8.67 \times 10^{-12} \text{ s}^{-1}$, respectively. The cross sections for Rb I are from the theoretical calculations of Weisheit (1972) for 1150 to 1250 Å, scaled to the measurements of Marr & Creek (1968) at longer wavelengths, while those for K I are from the measurements of Hudson & Carter (1965, 1967), Marr & Creek (1968), and Sandner et al. (1981). Since the ionization potentials for Rb I and K I are similar, 4.18 and 4.34 eV, there is no appreciable differential attenuation. We use this fact to account for Rb I absorption below 1150 Å; based on the total rate for K I, we applied a 13% ‘correction’ to $G(\text{Rb I})$. The result is a Rb/K ratio of $(1.3 \pm 0.3) \times 10^{-3}$ compared to the Solar System ratio of $(1.9 \pm 0.2) \times 10^{-3}$ (Anders & Grevesse 1989).

Limits or values of the Rb/K ratio are available from earlier studies of interstellar Rb as well. For the clouds toward σ Per, ζ Per, and ζ Oph, the most conservative limits on Rb I absorption (Federman et al. 1985) are used with our more recent determinations of the K I column density from the weak line at 4044 Å (Knauth et al. 2000, 2003). The 3- σ upper limits for $N(\text{Rb I})$ are $\leq 2.8 \times 10^9$, $\leq 1.9 \times 10^9$, and $\leq 3.7 \times 10^9 \text{ cm}^{-2}$, respectively. The limits on the Rb/K ratio then become $\leq 1.2 \times 10^{-3}$, $\leq 1.0 \times 10^{-3}$, and $\leq 1.8 \times 10^{-3}$. The Rb I detections toward Cyg OB2 Nos. 5 and 12 (Gredel et al. 2001) can be combined with results from high-resolution K I $\lambda 7699$ spectra (McCall et al. 2002). For the three main molecular components (+4.0, +6.5, and +12.3 km s⁻¹), we derive values for $N(\text{K I})$ of $9.4(7.7) \times 10^{11}$, $8.1(12) \times 10^{11}$, and $6.9(16) \times 10^{11} \text{ cm}^{-2}$ for the gas toward No. 5 (No. 12) when adopting a b -value of 1 km s⁻¹. The respective Rb/K ratios are 1.4×10^{-3} and 1.2×10^{-3} . (The uncertainties for these ratios are hard to quantify because the Rb I component structure is not known and because the K I column densities from $\lambda 7699$ are very susceptible to small changes in adopted b -value.) These comparisons suggest that the interstellar Rb/K ratio may be lower than the meteoritic abundance throughout the solar neighborhood.

4. Discussion

Insight into the nucleosynthesis of Rb is obtainable from the ratios $^{85}\text{Rb}/\text{K}$ and $^{87}\text{Rb}/\text{K}$ for the main 1.9 km s⁻¹ component toward ρ Oph A. We find $^{85}\text{Rb}/\text{K} = (0.73 \pm 0.12) \times 10^{-3}$ and $^{87}\text{Rb}/\text{K} = (0.60 \pm 0.13) \times 10^{-3}$, assuming that $G(\text{Rb I})$ and $\alpha(\text{Rb I})$ are not dependent on isotope. The Solar System ratios are $^{85}\text{Rb}/\text{K} = (1.37 \pm 0.14) \times 10^{-3}$ and $^{87}\text{Rb}/\text{K} = (0.53 \pm 0.06) \times 10^{-3}$. These ratios show that ^{85}Rb is underabundant in the gas by a factor of

about two, but ^{87}Rb has about the Solar System abundance. In other words, the $^{85}\text{Rb}/^{87}\text{Rb}$ and Rb/K ratios toward ρ Oph A are low because there is less ^{85}Rb . The ‘missing’ ^{85}Rb is comparable to predictions for the *r*-process component in stellar models (Beer et al. 1992; Raiteri et al. 1993), $\sim 65\%$. Moreover, the models (Beer et al. 1992; Raiteri et al. 1993; Arlandini et al. 1999) indicate that ^{87}Rb arises mainly from the *s*-process. We are led to believe that the lower interstellar abundance for ^{85}Rb is due to less *r*-process synthesis.

It is widely assumed that the site of the *r*-process is the very deep interior of a Type II supernova. Potassium is also a product of a SN II; it is synthesized in explosive oxygen burning (e.g., Clayton 2003). These different sites and quite different synthesis mechanisms make it likely that the *r*-process yield of a Rb isotope relative to the yield of K can vary; it may depend for example on the mass, metallicity, and rotation of a SN II’s progenitor.

The proposal that local interstellar gas may be deficient in *r*-process products relative to Solar System material is curiously supported by interstellar abundances of other lightly depleted or undepleted elements with a *r*-process contribution. We emphasize directions probing material toward Sco OB2, which includes ρ Oph A. For Solar System material, about 50% of Kr, 50% of Cd, and 30% of Sn are attributable to the *r*-process (Beer et al. 1992; Raiteri et al. 1993; Arlandini et al. 1999). The interstellar Kr abundance within a few hundred parsecs of the Sun is constant at 60% of the solar-wind value (Cartledge et al. 2001, 2003). Though there are fewer determinations of the interstellar Cd abundance, it is constant at 80% of the Solar System value (Sofia, Meyer, & Cardelli 1999). Sofia et al. find a Sn abundance that is essentially solar, if not slightly greater than solar, for sight lines showing little depletion in other elements. Arsenic, which is mostly *r*-process (Beer et al. 1992; Raiteri et al. 1993) and has only 1 isotope, is seen currently only in three reddened directions (Cardelli et al. 1993; Federman et al. 2003). It has a higher condensation temperature (see Cardelli et al. 1993) and thus it has more depletion, especially in reddened directions. Measurements of As II in lightly reddened sight lines, where little depletion is expected, appear necessary to confirm our hypothesis.

Variations in space and time of the mix of *s*- and *r*-process products in the Galaxy’s interstellar medium should be reflected in the abundances of the heavy elements in unevolved stars. Relative abundances of elements such as Sr, Y, and Zr and heavier elements such as Ba, Ce, and Eu for dwarfs of the thin disk do not vary from star to star by more than the measurement errors (Edvardsson et al. 1993; Chen et al. 2000; Reddy et al. 2003). These measurements would seem to exclude the larger variations expected for stars formed from gas with a large amplitude in the ratio of *s*- to *r*-process products. Our interstellar results suggest that differences in *n*-capture nucleosynthesis may be local to the solar neighborhood.

5. Concluding Remarks

Our estimate of the Rb isotope and the Rb/K ratios combined with the interstellar abundances of Kr, Cd, and Sn raise the intriguing possibility that the *r*-process products for such light *n*-capture elements are relatively underrepresented in the local interstellar medium relative to their contribution in the 4.5 Gyr older Solar System material. While models of the *s*-process are becoming quite sophisticated and generally give similar results, differences limit the ability to make definitive statements. For these rarer elements, the Solar System abundance is sometimes a matter of debate; Kr is an example. The precision of the atomic data is another factor. For Sn II, the *f*-values adopted by Sofia et al. (1999) are now known to be valid (Schechtman et al. 2000; Alonso-Medina, Colón, & Matínez 2003). A key test of our hypothesis is the measurement of accurate interstellar abundances for additional elements, particularly those derived mainly from the *r*-process.

We thank Dr. B. McCall, who kindly provided us with his K I spectra, and Dr. D. York for helpful suggestions. This work was supported in part by NASA LTSA grant NAG5-4957 to the Univ. of Toledo.

REFERENCES

Abia, C., Busso, M., Gallino, R., Dominguez, I., Straniero, O., & Isern, J. 2001, ApJ, 559, 1117

Abia, C., & Wallerstein, G. 1998, MNRAS, 293, 89

Alonso-Medina, A., Colón, C., & Martínez, C.H. 2003, ApJ, 595, 550

Anders, E., & Grevesse, N. 1989, Geochim. Cosmochim. Acta, 53, 197

Arlandini, C., Käppeler, F., Wissak, K., Gallino, R., Lugaro, M., Busso, M., & Straniero, O. 1999, ApJ, 525, 886

Beer, H., Walter, G., & Käppeler, F. 1992, ApJ, 389, 784

Cardelli, J.A., Federman, S.R., Lambert, D.L., & Theodosiou, C.E. 1993, ApJ, 416, L41

Cartledge, S.I.B., Meyer, D.M., & Lauroesch, J.T. 2003, ApJ, 597, 408

Cartledge, S.I.B., Meyer, D.M., Lauroesch, J.T., & Sofia, U.J. 2001, ApJ, 562, 394

Chen, Y.Q., Nissen, P.E., Zhao, G., Zhang, H.W., & Benoni, T. 2000, A&AS, 141, 491

Clayton, D. 2003, Handbook of Isotopes in the Cosmos – Hydrogen to Gallium (Cambridge: Cambridge Univ. Press)

Crutcher, R.M. 1978, *ApJ*, 219, 72

Edvardsson, B., Andersen, J., Gustafsson, B., Lambert, D.L., Nissen, P.E., & Tomkin, J. 1993, *A&A* 275, 101

Federman, S.R., Lambert, D.L., Sheffer, Y., Cardelli, J.A., Andersson, B.-G., van Dishoeck, E.F., & Zsargó, J. 2003, *ApJ*, 591, 986

Federman, S.R., Sneden, C., Schempp, W.V., & Smith, W.H. 1985, *ApJ*, 290, L55

Gratton, R.G., & Sneden, C. 1994, *A&A*, 287, 927

Gredel, R., Black, J.H., & Yan, M. 2001, *A&A*, 375, 553

Hudson, R.D., & Carter, V.L. 1965, *Phys. Rev.*, 139, A1426

—. 1967, *J. Opt. Soc. Am.*, 57, 1471

Jura, M., & Smith, W.H. 1981, *ApJ*, 251, L43

Käppeler, F., Beer, H., & Wissak, K. 1989, *Rep. Prog. Phys.*, 52, 945

Knauth, D.C., Federman, S.R., & Lambert, D.L. 2003, *ApJ*, 586, 268; erratum, 594, 664

Knauth, D.C., Federman, S.R., & Lambert, D.L. 2004, in preparation

Knauth, D.C., Federman, S.R., Lambert, D.L., & Crane, P. 2000, *Nature*, 405, 656

Lambert, D.L., & Luck, R.E. 1976, *Observatory*, 96, 100

Lambert, D.L. Smith, V.V., Busso, M., Gallino, R., & Straniero, O. 1995, *ApJ*, 450, 302

Lemoine, M., Ferlet, R., Vidal-Madjar, A., Emerich, C., & Bertin, P. 1993, *A&A*, 269, 469

Marr, G.V., & Creek, D.M. 1968, *Proc. R. Soc. London A*, 304, 233

McCall, B.J., et al. 2002, *ApJ*, 567, 391

Morton, D.C. 1991, *ApJS*, 77, 119

—. 2000, *ApJS*, 130, 403

Pan, K., Federman, S.R., Cunha, K., Smith, V.V., & Welty, D.E. 2003, submitted to *ApJ*

Péquignot, D., & Aldrovandi, S.M.V. 1986, A&A, 161, 169

Raiteri, C.M., Gallino, R., Busso, M., Neuberger, D., Käppeler, F. 1993, ApJ, 419, 207

Reddy, B.E., Tomkin, J., Lambert, D.L., & Allende Prieto, C. 2003, MNRAS, 340, 304

Sandner, W., Gallagher, T.F., Safinya, K.A., & Gounand, F. 1981, Phys. Rev. A, 23, 2732

Schectman, R.M., Cheng, S., Curtis, L.J., Federman, S.R., Fritts, M.C., & Irving, R.C. 2000, ApJ, 542, 400

Sofia, U.J., Meyer, D.M., & Cardelli, J.A. 1999, ApJ, 522, L137

Tomkin, J., & Lambert, D.L. 1999, ApJ, 523, 234

Tull, R.G., MacQueen, P.J., Sneden, C., & Lambert, D.L. 1995, PASP, 107, 251

Wane, S. 1985, J. Phys. B, 18, 3881

Wane, S., & Aymar, M. 1987, J. Phys. B, 20, 2657

Weisheit, J.C. 1972, Phys. Rev. A, 5, 1621

Welty, D.E., & Hobbs, L.M. 2001, ApJS, 133, 245

Table 1. Input Data and Results

| Species | λ (Å) | $F_l \rightarrow F_u$ | f -value | W_λ (mÅ) | N (cm $^{-2}$) |
|--------------------|-----------------------|---|------------------------------------|--|--|
| $^{85}\text{Rb I}$ | 7800.232 ^a | $2 \rightarrow 4, 3, 2, 1$ ^a | 2.90×10^{-1} ^a | $0.40 \pm 0.04(\text{obs}) \pm 0.07(\text{sys})$ | $(2.56 \pm 0.38) \times 10^9$ |
| | 7800.294 ^a | $3 \rightarrow 4, 3, 2, 1$ ^a | 4.06×10^{-1} ^a | $0.56 \pm 0.04(\text{obs}) \pm 0.07(\text{sys})$ | |
| $^{87}\text{Rb I}$ | 7800.183 ^a | $1 \rightarrow 3, 2, 1$ ^a | 2.61×10^{-1} ^a | $0.30 \pm 0.04(\text{obs}) \pm 0.07(\text{sys})$ | $(2.12 \pm 0.43) \times 10^9$ |
| | 7800.321 ^a | $2 \rightarrow 3, 2, 1$ ^a | 4.35×10^{-1} ^a | $0.40 \pm 0.04(\text{obs}) \pm 0.07(\text{sys})$ | |
| K I | 4044.143 ^b | ^c | 6.09×10^{-3} ^b | $1.19 \pm 0.09(\text{obs})$ ^d | $(1.38 \times 0.11) \times 10^{12}$ ^d |

^aMorton 2000.

^bMorton 1991.

^cHyperfine structure not resolved.

^dFor main component at 1.9 km s $^{-1}$.

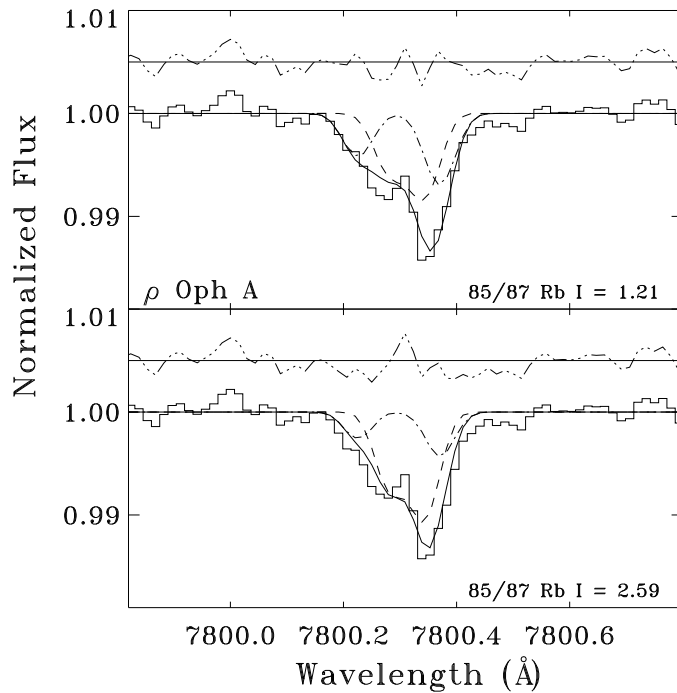


Fig. 1.— Rb I toward ρ Oph A. The best fit appears in the top panel, and a fit forcing the Rb isotope ratio to be the Solar System value is in the bottom panel. Notice the lack of agreement in the shoulders of the line in the lower panel. The dashed lines show the contributions from ^{85}Rb and the dot-dashed ones from ^{87}Rb . The line above each spectrum indicates data-fit, offset to 1.005.

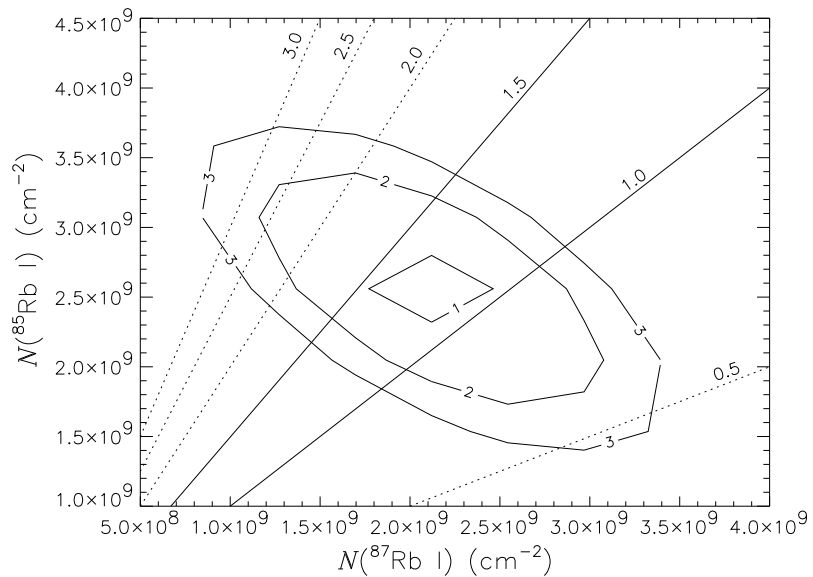


Fig. 2.— A map of chi-squared confidence levels for the best fit to Rb I absorption. Contours for 1, 2, and 3 sigma are shown. The straight lines shown as overlays represent different $^{85}\text{Rb}/^{87}\text{Rb}$ ratios.